I&EC research
Industrial & Engineering Chemistry Research

Article

pubs.acs.org/IECR

Selection of Controlled Variables for a Natural Gas to Liquids Process

Mehdi Panahi and Sigurd Skogestad*

Department of Chemical Engineering, Norwegian University of Science and Technology (NTNU), 7491 Trondheim, Norway

ABSTRACT: The aim of this work is to select the best individual or combined controlled variables (CVs) for a natural gas to hydrocarbon liquids (GTL) process based on the idea of self-optimizing control. The objective function is to maximize the variable income of the plant, and two modes of operation are studied. In mode I, where the natural gas flow rate is given, there are three unconstrained degrees of freedom (DOFs) and the corresponding individual self-optimizing CVs are selected as (i) CO_2 removal in fresh synthesis gas (syngas), (ii) CO mole fraction in fresh syngas, and (iii) CO mole fraction in recycle tail gas from the Fischer−Tropsch (FT) reactor. This set of CVs gives a worst-case loss of 1,393 USD/h. Adding one, two, and three measurements and controlling measurement combinations decrease the worst-case loss significantly, to 184, 161, and 53 USD/h, respectively. In mode II, the natural gas flow rate is a degree of freedom and it is optimal to increase it as much as possible to maximize profit. The variable income increases almost linearly until the oxygen flow rate becomes active. Practically, this is the maximum achievable income. Theoretically, it is possible to increase the natural gas flow rate to improve the objective function, but this results in large recycle flow rates to the FT reactor (similar to "snowballing") because its volume is the limitation.

1. INTRODUCTION

For large natural gas reservoirs, converting natural gas to transportable liquid fuels (GTL) is economical when the target markets are further than approximately 2500 km from the resources.[1] Figure 1 shows the gas commercialization options and situation of GTL processes compared to other possibilities of transportation, conversion, or usages.

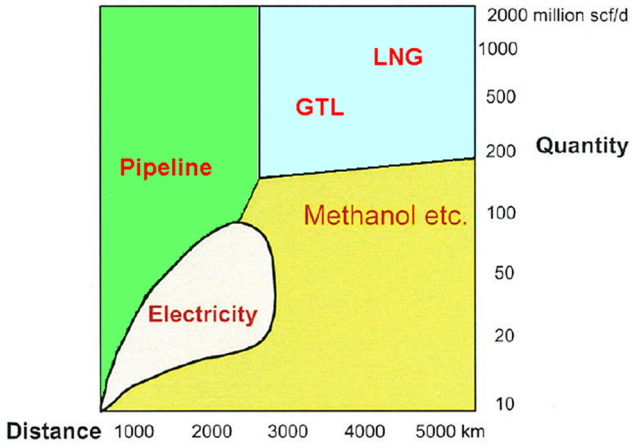

Figure 1. Gas commercialization options and situation of GTL processes.[1]

This paper is an extension of our previous work[2] which considered modeling and optimization of a GTL process, including degrees of freedom for operation and optimally active constraints. In the present paper, we consider in more detail how to implement operation, using the top-down part of the general plantwide control procedure of Skogestad.[3] We want to operate the plant economically efficient in the presence of unexpected disturbances. The main issue is, "which variables should be controlled?" To select the best controlled variables, the self-optimizing method is applied. "Self-optimizing control is when we can achieve an acceptable loss with constant set point values for the controlled variables (CVs) without the need to reoptimize when disturbances occur."[3] This means that we use off-line optimization and analysis to obtain a control structure that can use a constant set point policy for the CVs. This may completely remove the need for a real time optimization layer (RTO) for updating the set points when disturbances occur. However, at least theoretically, we will need to accept a small loss in objective cost compared to the case when RTO is used. By using measurement combinations, the loss can often be decreased significantly and from an engineering point of view close to zero. Based on the loss magnitude, one can decide on using individual or a combination of measurements as self-optimizing CVs.

In general, a different set of self-optimizing variables needs to selected in each operating region (set of active constraints), and in this paper we consider two modes of operation. In mode I, the feed rate to the process is given, and in mode II, the feed rate is adjusted to get the maximum possible profit.

The steps of the self-optimizing method are as follows:

Step 1. Define the objective function and constraints.

Step 2. Identify degrees of freedom (DOFs) for optimization.

Step 3. Identify important disturbances.

Step 4. Optimization for these disturbances.

Step 5. Identify candidate controlled variables (CVs).

Step 6. Select CVs.

In section 3, the self-optimizing steps are followed in detail for the GTL process to select the best controlled variables. The UniSim commercial simulator is used for modeling the process.

Received: November 20, 2011
Revised: May 22, 2012
Accepted: June 20, 2012
Published: June 20, 2012

   dx.doi.org/10.1021/ie202678h | *Ind. Eng. Chem. Res.* 2012, 51, 10179−10190

2. PROCESS DESCRIPTION

GTL processes include three main steps (see Figure 2) to convert natural gas to a range of liquid fuels. In the synthesis gas

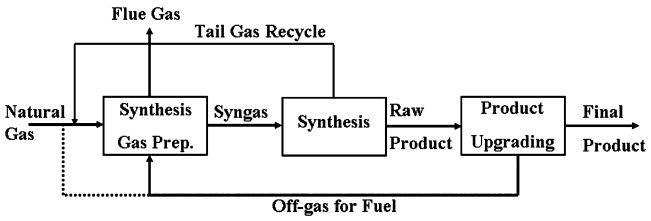

Figure 2. Simple flow sheet of GTL process.[4]

(syngas) unit, natural gas is reacted with oxygen and steam to produce "syngas", a mixture of CO and H_2. This is further converted to a range of liquid hydrocarbon fuels by the highly exothermic Fischer–Tropsch (FT) reactions.

The FT hydrocarbon products include mostly paraffins and olefins, in the range from light (methane) to heavy hydrocarbons (wax). In the final step, the heavier products are upgraded to clean fuels and the lighter hydrocarbons are recycled back to the syngas unit or used as fuel inside the plant.

The GTL flow sheet, process model, and nominal optimal data are taken from our previous work,[2] where more details are given. The syngas unit is assumed to operate at 30 bar. To simplify, we neglect the pressure drop for the individual equipment in the syngas unit, but we have included a pressure drop between the syngas unit and the FT reactor.[5] The pressure drop is nominally 3 bar and is simulated using a valve (V-1 in Figure 3) with a variable pressure drop as a function of flow rate. Figure 3 shows the process flow sheet with nominally optimal data. The syngas step consists of a pre-reformer, fired heater, and autothermal reformer (ATR), which is claimed to be the best way for syngas production.[6] The other main units are the CO_2 removal for the syngas stream and the FT reactor, which in our case is a cobalt based slurry bubble column reactor (SBCR).

2.1. Fired Heater and Pre-reformer. Fresh natural gas and recycled hydrocarbons from the FT unit are mixed and preheated in the fired heater to 455 °C[5] and then enter the pre-reformer. In the pre-reformer, all heavier hydrocarbons are converted by reaction with steam to syngas. The methanation and shift reactions are assumed to be in equilibrium in the pre-reformer.[7] The advantage of the pre-reformer is that one avoids cracking in the subsequent ATR. The outlet of the pre-reformer is further heated in the fired heater to 675 °C and then enters the ATR. To control the temperatures of the outlet streams of the fired heater, we use bypass streams (not shown in the flow sheet in Figure 3), which can be viewed as a control degree of freedom. In addition to preheating several streams, the fired heater produces superheated medium pressure (MP) steam which generates electric power for the oxygen plant and for the recycle compressors (compressors I and II in Figure 3).

2.2. Autothermal Reformer. The following reactions take place in the ATR:[8]

oxidation of methane:

$$CH_4 + \frac{3}{2}O_2 \leftrightarrow CO + 2H_2O \quad (1)$$

steam reforming of methane:

$$CH_4 + H_2O \leftrightarrow CO + 3H_2 \quad (2)$$

shift reaction:

$$CO + H_2O \leftrightarrow CO_2 + H_2 \quad (3)$$

In our simulations we assume pure oxygen is supplied from the air separation unit (ASU) although there are some impurities in practice from cryogenic ASU plants. The outlet of the ATR is

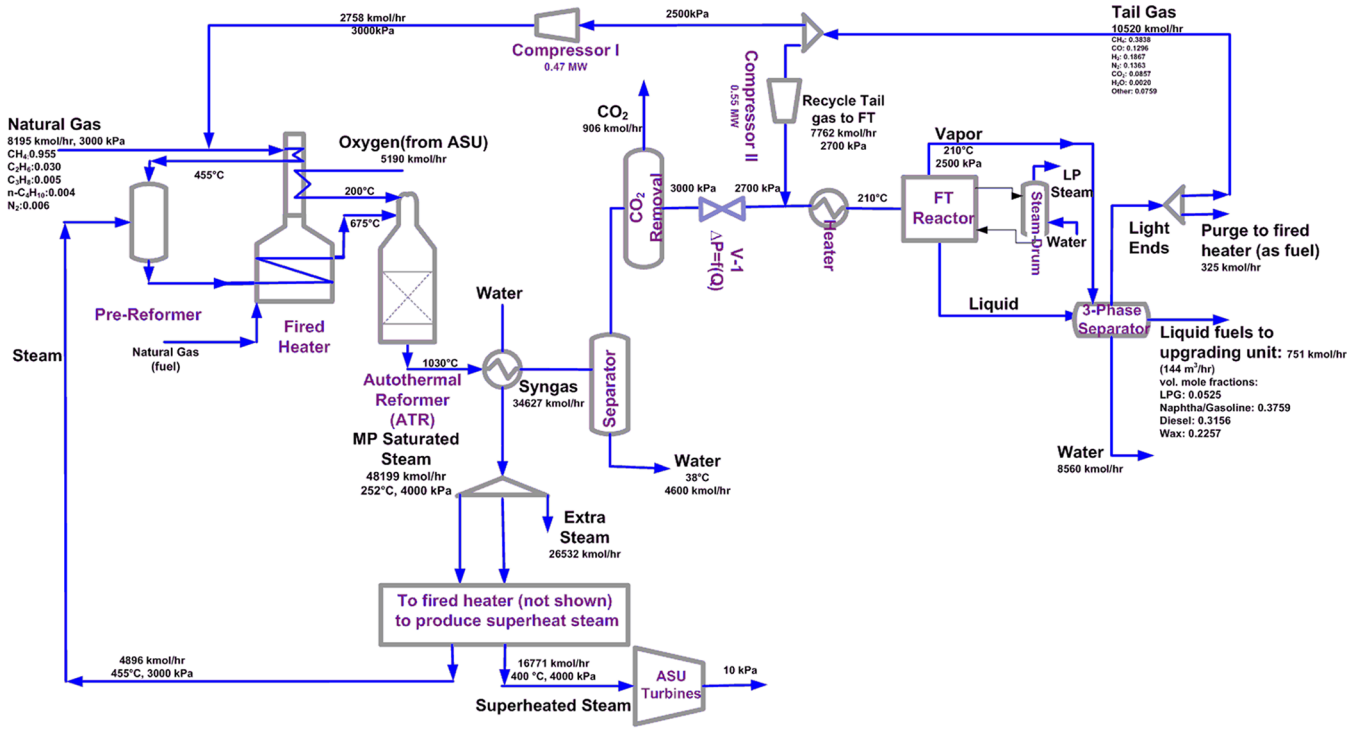

Figure 3. GTL flow sheet with data for optimal nominal point (mode I).

dx.doi.org/10.1021/ie202678h | Ind. Eng. Chem. Res. 2012, 51, 10179–10190

more than 1000 °C, and the heat is used to generate steam. The syngas is then further cooled to separate out associated water. In the next unit, the CO_2 content is reduced. This unit is not modeled in detail, but amine absorption/stripping could be an option. The prepared syngas, which we call the fresh syngas, has a H_2 to CO ratio of around 2 to 2.1. The exact ratio is decided by optimization.

2.3. Fischer−Tropsch (FT) Reactor. The volume of the FT reactor is assumed to be 2000 m^3 with a gas fraction of 40%.[5] The cooled FT reactor operates at 27 bar and 210 °C and UA = 19 255 kW/K, where U is the overall heat transfer coefficient and A is the heat transfer area. The FT reactions are highly exothermic, and an advantage of slurry reactors is their excellent heat removal properties. By controlling the boiling water pressure, the reactor temperature can indirectly be controlled. A compressor (compressor II in the flow sheet) was added in the FT recycle loop to compensate for the assumed 2 bar pressure drop in the FT reactor.

The highly exothermic FT reactions are described by Yates and Satterfield reactions.[9]

$$n\mathrm{CO} + 2n\mathrm{H_2} \rightarrow (-\mathrm{CH_2}-)_n + n\mathrm{H_2O} \tag{4}$$

where $n \geq 2$.The products are paraffins and olefins. Methane formation is also unavoidable. We use the proposed reaction rates of Iglesia et al.[10] for cobalt based FT reactions to simulate the slurry bubble column FT reactor (SBCR).

$$r_{\mathrm{CH_4}} = \frac{(1.08 \times 10^{-8})P_{\mathrm{H_2}}P_{\mathrm{CO}}{}^{0.05}}{1 + (3.3 \times 10^{-5})P_{\mathrm{CO}}}\left(\frac{\mathrm{mol_{CH_4}}}{\text{g-atom surface metal·s}}\right) \tag{5}$$

$$r_{\mathrm{CO}} = \frac{(1.96 \times 10^{-8})P_{\mathrm{H_2}}{}^{0.6}P_{\mathrm{CO}}{}^{0.65}}{1 + (3.3 \times 10^{-5})P_{\mathrm{CO}}}\left(\frac{\mathrm{mol_{CO}}}{\text{g-atom surface metal·s}}\right) \tag{6}$$

The details of the reaction rates and reactor simulation are given in our previous work.[2] The following lumps are assumed to describe the FT products: C_1, C_2, LPG (C_3−C_4), gasoline/naphtha (C_5−C_{11}), diesel (C_{12}−C_{20}), and wax (C_{21+}). Light ends (mostly C_1 and C_2) are either recycled to the syngas unit or purged to be used as fuel for the fired heater. The Anderson−Schultz−Flory (ASF) model is used to describe the distribution of the products.

$$w_n = n(1 - \alpha)^2\alpha^{n-1} \tag{7}$$

Here w_n is the weight fraction of hydrocarbons (C_n) and α is the chain growth probability. Figure 4 illustrates the meaning of chain growth probability.

As Figure 4 shows, the selectivity to hydrocarbons is a function of the chain growth probability. The factor α is a function of the hydrogen to carbon monoxide ratio. In previous work we discussed these dependencies[2] and showed how significant this ratio is. We use the function proposed by Yermakova and Anikeev[11] and modified by Song et al.[12] to calculate chain growth probability:

$$\alpha = \left(0.2332\frac{y_{\mathrm{CO}}}{y_{\mathrm{CO}} + y_{\mathrm{H_2}}} + 0.633\right)[1 - 0.0039(T - 533)] \tag{8}$$

Here, y_{CO} and $y_{\mathrm{H_2}}$ are mole fractions in the FT reactor and T is the reactor temperature (kelvin).

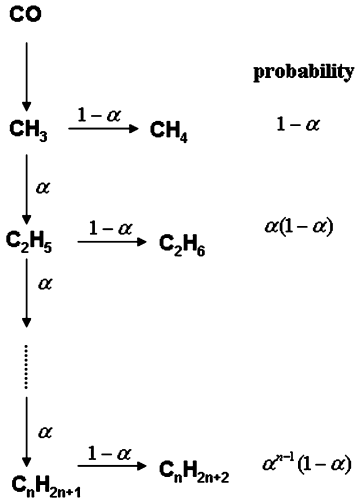

Figure 4. Probability of the chain growth to hydrocarbons in FT reactions.[1]

To summarize the FT reaction loop, note that syngas is converted to a range of hydrocarbons through highly exothermic reactions where the conversion of reactions is dependent on the ratio of H_2 to CO, the temperature and pressure of the reactor, the amount, density, and selectivity of the catalyst, the volume of the reactor, and the total mass flow entering the reactor.

In section 3, we apply the self-optimizing method[3] to select the best individual and combined self-optimizing CVs for this process.

3. TOP-DOWN ANALYSIS FOR OPERATION OF THE GTL PROCESS

We perform the analysis in two modes of operation: in mode I, the natural gas feed flow rate is given (disturbance); in mode II, the natural gas feed flow rate is a degree of freedom for optimization.

Table 1. Assumed Prices for Costs[2]

raw materials:

- natural gas: 0.5 USD/MMBtu
- water and steam: 0
- oxygen: Oxygen is supplied by the ASU unit and we assume that the GTL plant supplies the required steam for the oxygen plant. The price we need to pay decreases somewhat with increased oxygen usage:

$$P_{\mathrm{O_2}} = P^{\circ}_{\mathrm{O_2}}\left(\frac{\dot{m}_{\mathrm{O_2}}}{\dot{m}^{\mathrm{ref}}_{\mathrm{O_2}}}\right)^{-0.3}, \qquad P^{\circ}_{\mathrm{O_2}} = 0.11 \text{ USD/kg} \tag{11}$$

energy: 0 (the required energy is supplied internally by heat integration)

CO_2 removal: 50 USD/ton of CO_2

products:

- LPG (C_3−C_4) = 0.9 USD/kg
- gasoline/naphtha (C_5−C_{11}) = 0.73 USD/kg
- diesel (C_{12}−C_{20}) = 0.71 USD/kg
- wax (C_{21+}) = 0.63 USD/kg

3.1. Mode I: Natural Gas Flow Rate Is Given. The steps of the top-down analysis are as follows.

Step 1. Define the Objective Function and Constraints. We define variable income (profit) as the objective function to be maximized.

$$\text{variable income} = \text{sales revenue} - \text{variable cost} \tag{9}$$

dx.doi.org/10.1021/ie202678h | Ind. Eng. Chem. Res. 2012, 51, 10179−10190

Table 2. Optimal Nominal Values

H_2O/C	O_2/C	CO_2 removal (%)	recycle ratio to FT (%)	purge of tail gas (%)	H_2O/C fresh	H_2O/C into FT	CO conversion (%) per pass	CO conversion (%) overall	H_2 conversion (%) per pass	H_2 conversion (%) overall	α	carbon efficiency (%)	obj function (USD/h)
0.6010	0.5233	75.73	73.79	3	2.1	2.03	85.74	95.50	89.93	96.92	0.87	74.59	49,293

Table 3. Possible Pairings of Steady-State Degrees of Freedom with Equality/Active Controlled Variables

degree of freedom (DOF)	controlled variable (CV)
1. superheat steam bypass in fired heater	superheat steam temperature to pre-reformer
2. natural gas feed rate as fuel (makeup) to the fired heater	outlet temperature of fired heater (active constraint)
3. natural gas + recycle hydrocarbon bypass in fired heater	natural gas + recycle hydrocarbon feed temperature to pre-reformer
4. oxygen feed rate to ATR	ATR outlet temperature (active constraint)
5. oxygen bypass in fired heater	oxygen feed temperature to ATR
6. cooling duty for water removal from fresh syngas	separator temperature
7. preheater duty for FT reactor	FT reactor inlet temperature
8. steam (LP) flow rate for FT reactor cooling	steam drum pressure
9. three-phase separator cooling duty	three-phase separator temperature
10. compressor II duty (recycle tail gas flow to FT reactor)	compressor II outlet pressure
11. recycle tail gas purge ratio	purge ratio (active constraint)
12. compressor I duty (recycle tail gas flow to syngas unit)	compressor I outlet pressure

Table 4. Five Best Sets of Individual Self-Optimizing CVs in the Optimal Nominal Case (Mode I of Operation)

no.	set			loss (USD/h)
1	y_3: CO_2 removal	y_9: CO mole fraction in fresh syngas	y_{12}: CO mole fraction in tail gas	1,393
2	y_3: CO_2 removal	y_2: H_2O/C	y_6: H_2/CO in tail gas	1,457
3	y_3: CO_2 removal	y_2: H_2O/C	y_5: H_2/CO in fresh syngas	1,698
4	y_3: CO_2 removal	y_6: H_2/CO in tail gas	y_5: H_2/CO in fresh syngas	2,594
5	y_{10}: CH_4 mole fraction in fresh syngas	y_6: H_2/CO in tail gas	y_5: H_2/CO in fresh syngas	2,643

Table 5. Nonlinear Analysis of the Proposed Self-Optimizing Structure and Corresponding Loss

	loss (USD/h)
d_1: 10% increase in natural gas feed rate	88
d_2: 10% decrease in natural gas hydrocarbon mole fractions (increase in N_2 mole fraction (and corresponding decrease in hydrocarbons)	359
d_3: 25 °C decrease in fired heater outlet temperature	44

$$\text{variable cost} = \text{cost of raw materials} + \text{cost of energy} + \text{cost of } CO_2 \text{ removal} \quad (10)$$

The prices for raw materials, products, and other costs are given in Table 1.[2] Most of the required energy is supplied internally by heat integration or by excess steam; therefore, we did not include the cost for energy. Correspondingly, no credit was assumed for steam generated in the process (MP steam in boiler after ATR, low pressure (LP) steam in FT reactor). We expect that this assumption will not affect our control structures. For the CO_2 removal unit costs, in the presence of extra steam in the plant, the required energy for regenerating of solvent can be easily supplied. Anyway, we have included 50 USD/ton CO_2 in the optimization.

The inequality constraints are as follows.

1. The feed syngas molar ratio $H_2O/C \geq 0.3$ to ensure soot-free conditions. Carbon in this ratio includes fresh and recycled hydrocarbons. Note that Holdor Topsøe reports soot free operations at even lower values,[6] but we choose 0.3 as the lower bound.
2. The inlet temperature of the ATR (outlet of fired heater) $\leq$ 675 °C. The reason for this limit is piping material constraint.[13]
3. The outlet of ATR $\leq$ 1030 °C. This temperature is an average of several ATR temperatures reported by Holdor Topsøe[14] which ensures soot-free operation.
4. To avoid a convergence problem, for simulation purposes, the purge ratio of tail gas is bounded at 3% although the optimal is a lower value at around 2%. The purpose of the purge stream is to get rid of the nitrogen entering the fresh natural gas feed.
5. In addition, there are capacity constraints on the variable units: fired heater (duty +40% compared to nominal), CO_2 removal unit (+20% feed rate), and oxygen plant (+20% oxygen flow rate).

The equality constraints, most of which were explained in the process description, are the following:

1. The fresh natural gas + recycle hydrocarbon temperature to the pre-reformer is kept at 455 °C.
2. The steam temperature to the pre-reformer is kept at 455 °C.
3. The oxygen feed temperature to the ATR is kept at 200 °C.
4. The feed enters the syngas unit at 30 bar. Note that the pressure of the fresh streams are set in other units which are outside our flow sheet boundary.
5. The fresh syngas from the ATR (after passing the boiler) is cooled to 38 °C for separation of water content.
6. The syngas enters into the FT reactor at 210 °C.
7. The boiling water pressure (cooling medium of the FT reactor) is kept at 12.5 bar (low pressure (LP) steam) to indirectly control the FT reactor temperature. This gives a gradient of 20 °C between the FT desired temperature (210 °C) and the coolant (190 °C).
8. FT products are cooled to 30 °C in a three-phase separator to separate liquid fuels, water, and tail gas.
9. The recycle tail gas to FT reactor is compressed to 27 bar.

dx.doi.org/10.1021/ie202678h | Ind. Eng. Chem. Res. 2012, 51, 10179−10190

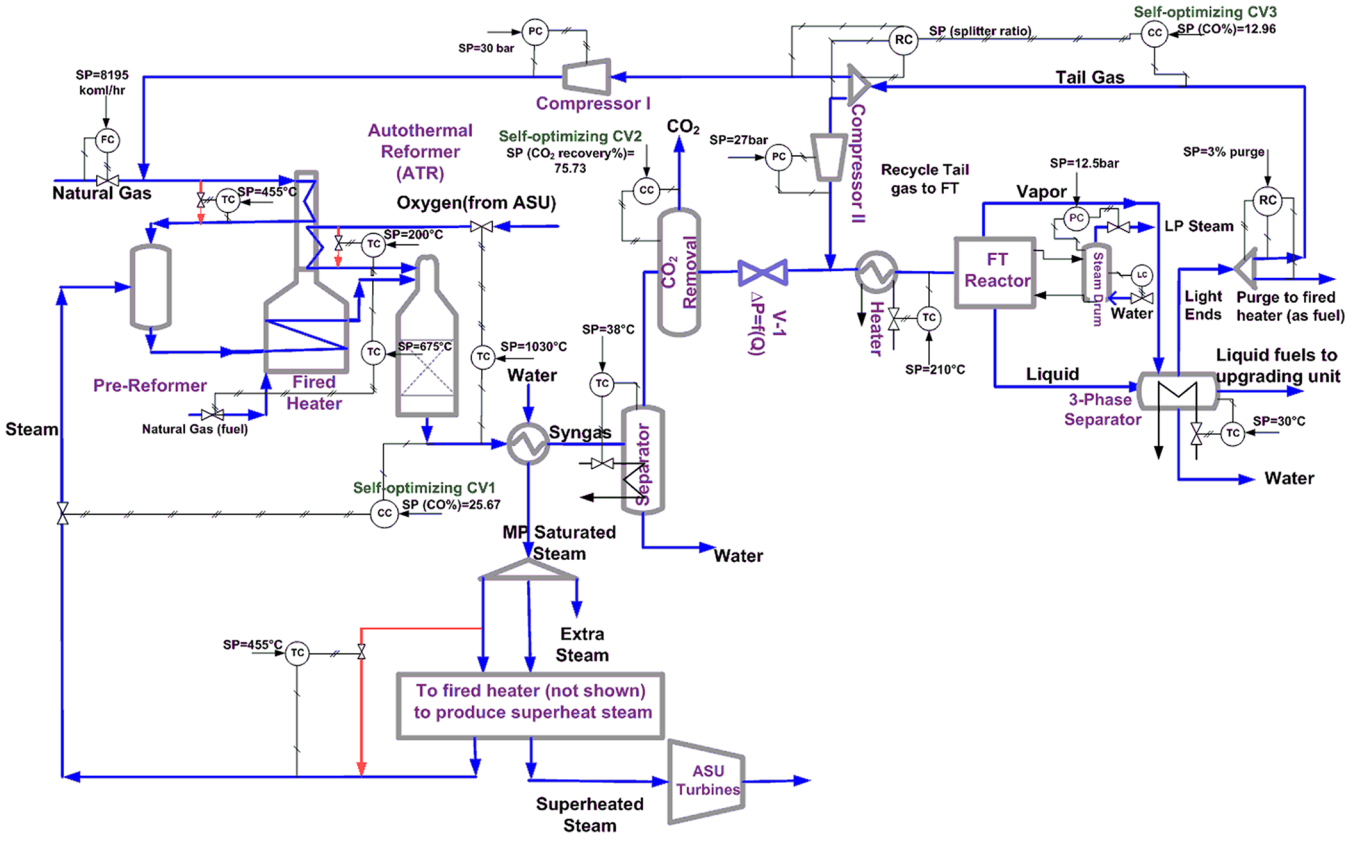

Figure 5. Possible control structure for the steady-state degrees of freedom for mode I of operation. (Red lines are bypass streams.) Note that we are considering the selection of steady-state CVs, so we are not concerned with inventory control. The inventory loops on the flow sheet, including pressure control, are included for steady-state simulation purposes and do not necessarily correspond to the actual loops. For example, in practice, the pressure in the FT reactor may be controlled using the purge flow, and the purge two split ratios should be controlled using compressors I and II. Also, the actual valve for controlling the split would be on the purge flow because we do not want any valves in the gas recycle, but again it would give the same result at steady state.

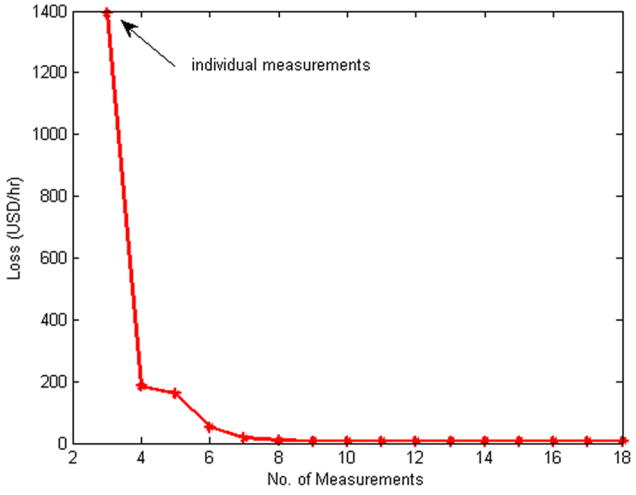

Figure 6. Minimum worst-case loss with different numbers of measurements (mode I).

Step 2. Identify Degrees of Freedom (DOFs) for Optimization. There are 15 main steady-state operational degrees of freedom which can be selected (the reader is referred to our previous work[2] for a detailed discussion):

1. H_2O (superheat steam) feed rate to pre-reformer (this can be viewed also as the ratio H_2O/C)
2. superheat steam bypass in fired heater
3. natural gas feed rate as fuel (makeup) to the fired heater
4. natural gas + recycle hydrocarbon bypass in fired heater
5. oxygen feed rate to ATR
6. oxygen bypass in fired heater
7. cooling duty for water removal from fresh syngas
8. CO_2 removal
9. preheater duty for FT reactor
10. steam (LP) flow rate for cooling FT reactor
11. three-phase separator cooling duty for separation of FT products
12. recycle ratio to FT reactor, which is the percentage of recycled tail gas that enters the FT reactor (The rest is recycled back to the syngas unit (pre-reformer).)
13. compressor II duty (recycle tail gas flow to FT reactor)
14. recycle tail gas purge ratio
15. compressor I duty (recycle tail gas flow to syngas unit)

Step 3. Identification of Important Disturbances. The main disturbances (d) from an industrial point of view are variations in the natural gas feed rate, natural gas composition, and natural gas price. We also include a variation in the FT "kinetic parameter" to include the effect of model mismatch in FT reactions in our analysis. In addition, the value of all active constraints may be considered as disturbances (see the optimization part further for final selection of the active constraints). We determine the maximum expected value for each disturbance in step 6.

Step 4. Optimization. We first did the optimization for the nominal case using the "Mixed method" in UniSim. This method

dx.doi.org/10.1021/ie202678h | Ind. Eng. Chem. Res. 2012, 51, 10179−10190

Table 6. Optimal Measurement Combinations (CVs) with Corresponding Losses (Mode I)

no. measurements	optimal CVs	worst-case loss (USD/h)
3	$CV1 = y_3$ $CV2 = y_9$ $CV3 = y_{12}$	1,393
4	$CV1 = 0.0979y_3 - 7.8012y_8 + 6.0855y_{14} - 14.0955y_{15}$ $CV2 = 0.5675y_3 + 1.7998y_8 + 1.4682y_{14} - 4.4740y_{15}$ $CV3 = -1.3208y_3 + 18.8916y_8 + 0.0933y_{14} - 6.9939y_{15}$	184
5	$CV1 = 0.1051y_3 + 0.4706y_6 - 7.8432y_8 - 1.9028y_{11} + 2.2211y_{15}$ $CV2 = 0.5991y_3 + 0.1158y_6 + 1.4006y_8 - 0.8808y_{11} + 0.0283y_{15}$ $CV3 = -1.3865y_3 + 0.0022y_6 + 19.7495y_8 + 0.9013y_{11} - 7.9914y_{15}$	161
6	$CV1 = -1.2398y_3 + 5.4289y_6 - 16.6155y_7 + 8.2854y_8 - 16.7099y_{11} + 40.2823y_{15}$ $CV2 = 0.4956y_3 + 0.4974y_6 - 1.2787y_7 + 2.6418y_8 - 2.0204y_{11} + 2.9575y_{15}$ $CV3 = -1.7597y_3 + 1.3781y_6 - 4.6106y_7 + 24.2249y_8 - 3.2075y_{11} + 2.5700y_{15}$	53
7	$CV1 = -2.0063y_2 - 2.2283y_3 + 6.1392y_6 - 22.7731y_7 + 6.2647y_8 - 17.2959y_{11} + 22.1873y_{14}$ $CV2 = -1.4081y_2 - 0.0565y_3 + 1.2053y_6 - 3.2276y_7 - 0.3196y_8 - 3.1263y_{11} + 3.6418y_{14}$ $CV3 = 1.4675y_2 - 1.2323y_3 + 0.6431y_6 - 3.3250y_7 + 27.8493y_8 - 2.0504y_{11} - 0.9377y_{14}$	17

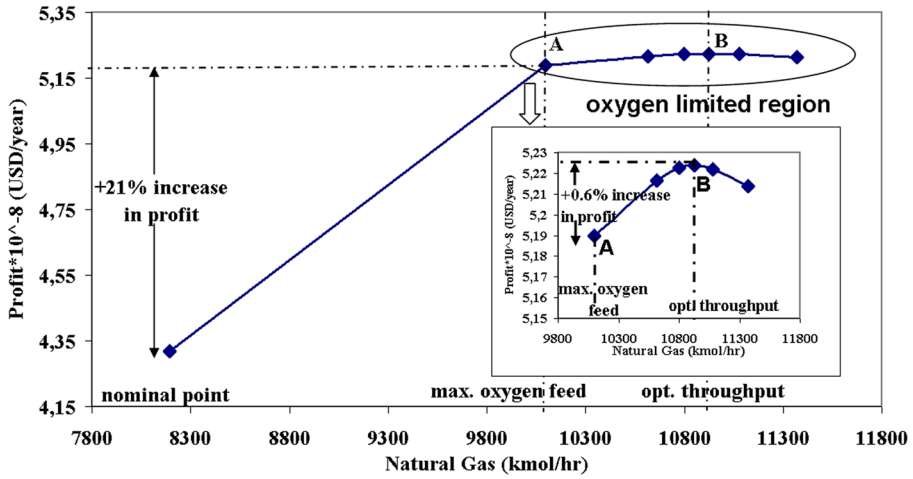

Figure 7. Optimal profit as a function of natural gas flow rate. Point A; near maximum profit (recommended operating point); point B, maximum achievable profit (optimal throughput).

tries to combine the advantage of global optimization of the BOX method and the efficiency of the SQP method. Initially, it uses the BOX method with a very loose convergence tolerance and then switches to the SQP method to locate the final solution with the desired tolerance.[15] Figure 3 shows the optimal nominal flow sheet. Table 2 shows the optimal nominal values of some of the important parameters. The "carbon efficiency" in Table 2 is the ratio of the carbon in the produced hydrocarbons to the carbon in the feed natural gas, including the required natural gas as fuel in the fired heater.

We find three active constraints during optimal nominal operation:

1. The outlet temperature of the fired heater is active at the maximum (675 °C).
2. The outlet temperature of the ATR is active at the maximum (1030 °C).
3. The purge ratio is active at the specified minimum, which is to purge 3% of the tail gas.

Since change at any of these active constraints has a significant effect on the objective function value,[2] we included all of them as disturbances during analysis.

We have 15 steady-state degrees of freedom, 9 equality constraints, and 3 active constraints, which each needs one degree of freedom for control. Therefore, we have 3 (=15 − 9 − 3) remaining unconstrained degrees of freedom.

dx.doi.org/10.1021/ie202678h | Ind. Eng. Chem. Res. 2012, 51, 10179−10190

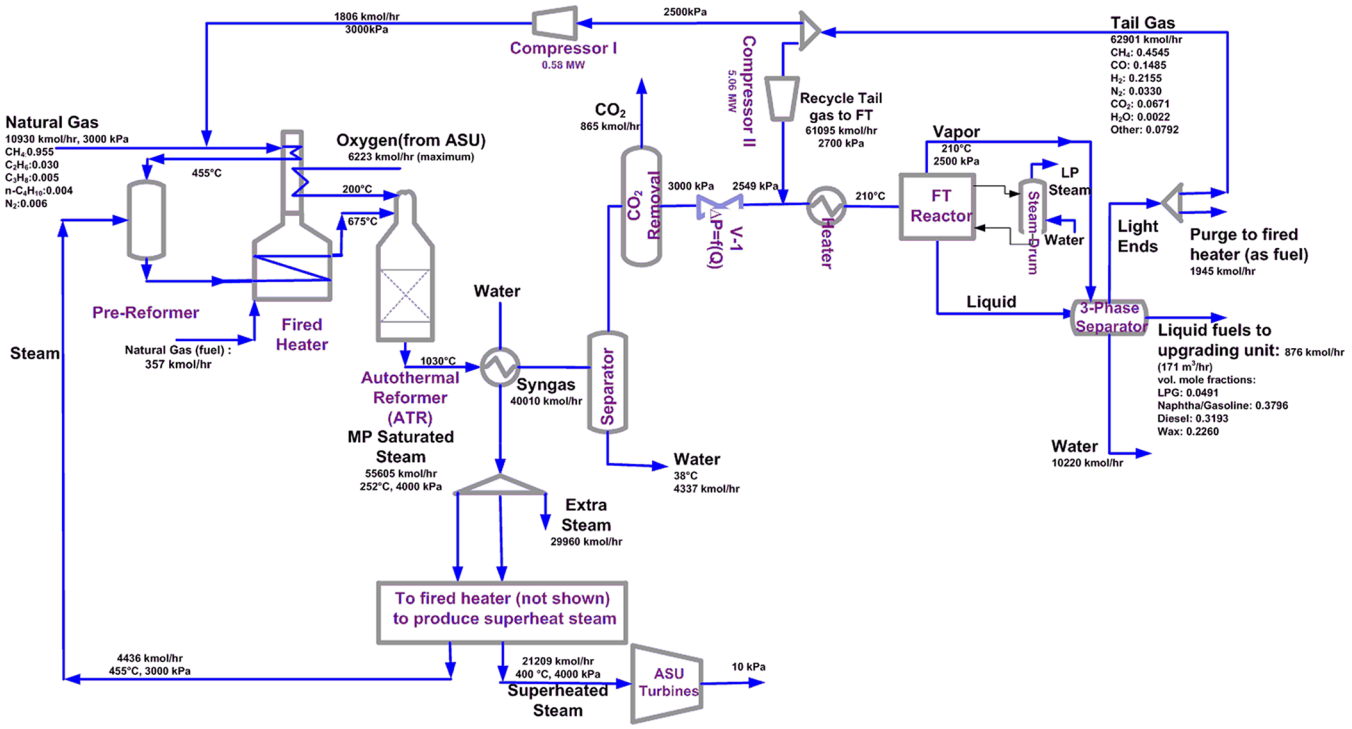

Figure 8. GTL flow sheet with data for optimal throughput (mode II, point B).

Unconstrained CVs in Mode I. There are many ways to pair the constraints with the degrees of freedom (inputs), but with the suggested pairings in Table 3, we are left with the following unconstrained degrees of freedom: u_1, the feed H_2O/C; u_2, the CO_2 removal percent before the FT reactor; and u_3, the recycle ratio to the FT reactor.

The objective is now to select the best three self-optimizing CVs to pair with these DOFs. Note that the actual choice of unconstrained degrees of freedom (u_1, u_2, u_3) does not really matter and we would have obtained equivalent results with other choices, although the matrices G^y, G^y_d, J_{uu}, and F in the subsequent analysis would be different.

Step 5. Identification of Candidate Controlled Variables. We consider 18 candidate measurements including the three unconstrained degrees of freedom (actually, all 15 DOFs could have been considered, but we only consider these three):

1. O_2/C (y_1)
2. feed $H_2O/C = u_1$ (y_2)
3. CO_2 removal % = u_2 (y_3)
4. recycled tail gas ratio to FT reactor = u_3 (y_4)
5. H_2/CO in fresh syngas (y_5)
6. H_2/CO in tail gas (y_6)
7. H_2/CO into FT reactor (y_7)
8. H_2 mole fraction in fresh syngas (y_8)
9. CO mole fraction in fresh syngas (y_9)
10. CH_4 mole fraction in fresh syngas (y_{10})
11. H_2 mole fraction in tail gas (y_{11})
12. CO mole fraction in tail gas (y_{12})
13. CH_4 mole fraction in tail gas (y_{13})
14. H_2 mole fraction into FT reactor (y_{14})
15. CO mole fraction into FT reactor (y_{15})
16. fresh syngas flow rate (y_{16})
17. tail gas flow rate to syngas unit (y_{17})
18. tail gas flow rate to FT reactor (y_{18})

This is not a complete list, but it includes some of the most obvious and practical candidates to measure and control. We have 18 candidate measurements, and one needs to select three individual measurements, CV = Hy, where H is the selection matrix. Therefore there are

$$\binom{18}{3} = \frac{18!}{3!15!} = 816$$

possible single measurement candidate sets. The self-optimizing method is applied in the next step to choose the best set.

Step 6. Selection of CVs. To find the best set of CVs, we applied the "exact local method",[16] which gives the maximum loss imposed by each candidate set in the presence of disturbances and measurement noise. The set with the minimum worst-case loss is the best. Expressions 12−15 give the mathematical formulation of calculating loss.

$$\text{worst-case loss} = \frac{1}{2}\bar{\sigma}(M)^2 \tag{12}$$

$$M = J_{uu}^{1/2}(HG^y)^{-1}(H[FW_d \quad W_n]) \tag{13}$$

where the optimal sensitivity (F) can be obtained analytically from (14) or numerically by reoptimizing the process from (15).

$$F = G^y J_{uu}^{-1} J_{ud} - G^y_d \tag{14}$$

$$F = \frac{\Delta y^{\text{opt}}}{\Delta d} \tag{15}$$

In (12), $\bar{\sigma}(M)$ is the maximum singular value of matrix M, J_{uu} is the Hessian of the objective function with respect to unconstrained DOFs, G^y is the gain of the selected measurements from the inputs, W_d is the expected magnitude of the disturbances, W_n is the implementation error, J_{ud} is the second derivative of the objective function with respect to DOFs and disturbances, and G^y_d is the gain from disturbances to the selected measurements. It

dx.doi.org/10.1021/ie202678h | Ind. Eng. Chem. Res. 2012, 51, 10179−10190

Table 7. Optimal Values at Three Operating Points

	feed H_2O/C	O_2/C into ATR	CO_2 removal (%)	recycle ratio to FT (%)	purge of tail gas (%)	H_2/CO fresh syngas	H_2/CO into FT	CO conversion (%) per pass	CO conversion (%) overall	H_2 conversion (%) per pass	H_2 conversion (%) overall	α	carbon efficiency (%)	compressor II (duty, MW)	obj function (USD/h)
opt. nominal	0.6010	0.5233	75.73	73.79	3	2.1	2.03	85.74	95.50	89.93	96.92	0.8707	74.59	0.55	49,293
max oxygen (A)	0.5357	0.5160	76.80	90	3	2.092	1.91	67.08	94.14	74.705	95.88	0.8692	74.30	2.15	59,246
opt. throughput (B)	0.4084	0.5040	76.04	97.13	3	2.095	1.80	51.25	94.79	60.69	96.39	0.8701	74.31	5.06	59,634

is worth knowing that the Frobenius norm, which gives the average loss, could be used instead of worst-case loss, but both methods give the same results.[17]

We consider seven disturbances (d) with the following maximum expected magnitude (included in the diagonal matrix, W_d):

d_1 (natural gas (NG) flow rate): 10%
d_2 (NG hydrocarbon composition): 10%; the disturbance d_2 is an increase in N_2 mole fraction (and corresponding decrease in hydrocarbons) (In the analysis it was set at 10% (W_d), but in the simulation we only used 3%.)
d_3 (fired heater outlet temperature): 30 °C
d_4 (ATR outlet temperature): 40 °C
d_5 (FT reaction rate constant): 10%
d_6 (purge ratio): 15%
d_7 (NG price): 10%

The implementation error (measurement noise) for the candidate measurements is assumed to be (included in the diagonal matrix, W_n) the following: compositions, 0.1%, flow rates, 10%, split ratios, 15%.

Individual Measurements as CVs. A branch and bound algorithm[18] is applied to find the best set of single measurements with the minimum worst-case loss. Table 4 shows the five best sets with their corresponding worst-case losses. The smallest loss is obtained by controlling the CO_2 removal (y_3) in the CO_2 removal unit, the CO mole fraction in the fresh syngas (y_9), and the CO mole fraction in the tail gas (y_{12}).

We pair the CVs of the best set with the corresponding close-by manipulated variables: CV1 = CO mole fraction in outlet of the ATR (y_9) is controlled using u_1 = feed H_2O/C. CV2 = CO_2 removal % (y_3) is controlled using u_2 = CO_2 removal plant. CV3 = CO mole fraction in tail gas (y_{12}) is controlled using u_3 = recycle tail gas ratio to the FT reactor. The resulting control structure is shown in Figure 5. The CV2 "pairing" seems strange, but it follows because we have not modeled in detail the CO_2 unit, so the input (u_2) is actually a CV (y_3). The demonstrated control loop just determines that the CO_2 removal percentage is controlled internally by the CO_2 removal plant. Manipulating of recycle amine in case an amine absorption/stripping system is applied will be one possibility for controlling the CO_2 removal.

The self-optimizing method is based on a linear analysis; therefore, a nonlinear analysis for selected CVs is required. The three self-optimizing CVs are kept constant in their optimal nominal points using the suggested pairings in the flow sheet and then the disturbances d_1, d_2, and d_3 are implemented as mentioned in Table 5. In addition, the flow sheet is reoptimized for each disturbance to find the corresponding economic loss. In all cases the flow sheet converges without reaching a new constraint. Similar conclusions from other disturbances are expected. Loss values are also all smaller than the maximum worst-case loss (1,393 USD/h) given by the analysis.

Measurement Combinations as CVs. As the loss of the best individual sets of measurements in Table 4 is fairly high (compared to the objective function value in the optimal nominal point), we consider measurement combinations as CVs, CV = Hy, where H is a "full matrix" in terms of the selected measurements, to get a smaller loss.[19] The optimal H is obtained by solving the following optimization problem.

$$\min_H \|HY\|_F^2 \quad \text{s.t.} \quad HG^y = J_{uu}^{1/2} \tag{16}$$

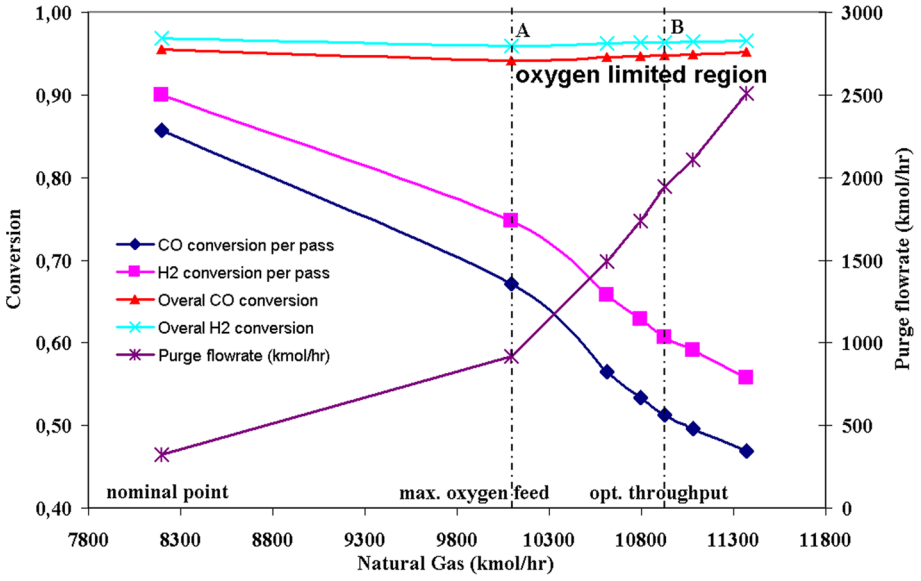

Figure 9. Optimal values of CO and H_2 conversion (single pass and overall) in FT reactor and purge flow rate as function of natural gas feed rate.

Table 8. Five Best Sets of Individual Self-Optimizing CVs in the Optimal Throughput Case (Mode II, Point B)

	set			
no.				loss (USD/h)
1	y_3: CO_2 removal	y_2: H_2O/C	y_7: H_2/CO into FT reactor	3,022
2	y_3: CO_2 removal	y_2: H_2O/C	y_6: H_2/CO in tail gas	3,316
3	y_3: CO_2 removal	y_2: H_2O/C	y_5: H_2/CO in fresh syngas	3,495
4	y_3: CO_2 removal	y_2: H_2O/C	y_{17}: tail gas flow rate to syngas unit	4,179
5	y_3: CO_2 removal	y_9: CO mole fraction in fresh syngas	y_{15}: CO mole fraction into FT reactor	4,419

where $Y = [FW_d \quad W_n]$. An analytical solution[19] for (16) is

$$H^T = (YY^T)^{-1}G^y(G^{yT}(YY^T)^{-1}G^y)^{-1}J_{uu}^{1/2}$$

A partial branch and bound algorithm[20] is applied to find the best set of CVs with more measurements than three. Figure 6 and Table 6 show the results of solving (12) and (16) for different numbers of measurements.

The results show that by having four measurements the loss decreases significantly from 1,393 to 184 USD/h and by having five and six measurements the loss decreases further to 161 and 53 USD/h, respectively. By combining seven measurements the best worst-case loss is 17 USD/h, which is almost 0 from a practical point of view. Measurement y_3 (CO_2 removal) is always included, but the other measurements in the optimal set vary. One disadvantage of measurement combinations is the lack of physical meaning. Also, dynamic issues, such as inverse response, may cause problems for control, and it may be necessary to use cascade control. It is recommended to perform dynamic simulations to test the practicality of the selected combined CVs.

3.2. Mode II: Natural Gas Feed Is a Degree of Freedom for Optimization. From an economical point of view with the given prices, it is optimal to increase the amount of natural gas feed as much as possible to get more profit. As mentioned earlier, the following maximum capacity constraints are included:

- duty of fired heater: +40% compared to nominal in mode I
- feed rate to CO_2 removal unit: +20%
- oxygen feed rate: +20%

We did not include any upper bound on the compressor duties. This is because in mode I the nominal compressor duties (compressor I, 0.47 MW; compressor II, 0.55 MW) are small compared with the duty of the fired heater (energy duty, 328.6 MW), so we may consider basing the design capacity for the compressors on the mode II operation.

The profit is shown as a function of the feed rate in Figure 7. In addition to the oxygen flow rate, the outlet temperature of the fired heater (at maximum), the outlet temperature of the ATR (at maximum), and the purge ratio (at minimum) are also active; they are the same active constraints as in the nominal case. The profit increases almost linearly with the natural gas flow rate (see Figure 7) up to the point when the first capacity constraint is reached, which is when the oxygen flow rate reaches its maximum (point A in Figure 7). At this point the increase in natural gas feed rate is +23.18% (compared to the nominal point). The reason it does not increase completely linearly is because of the fixed volume of the FT reactor, which implies that the optimal values of the intensive variables change somewhat.

The feed rate can be increased further to +33.32% (point B in Figure 7), at which we reach the bottleneck where a further increase gives infeasible operation. Figure 8 shows the optimal flow sheet at the optimal throughput. Table 7 summarizes the optimal values of the main parameters. However, note from Figure 7 and Table 7 that although the profit increases by +21.0% from the nominal point to point A, it only has a very small further increase to +21.6% in point B. Thus, in practice, operating point A may actually be the optimal, because in point B the compressor work is about twice as large as in point A. The compressor work is included in our economic optimization, but the minor operational economic benefit in point B may not justify the extra capital costs of a larger compressor. Also, there are other operational disadvantages with large variations in the recycle flow ("snowballing") and there is also the issue of less effective use of resources in point B since the purge flow is large. Nevertheless, we choose to work with operating point B for the further control studies.

dx.doi.org/10.1021/ie202678h | Ind. Eng. Chem. Res. 2012, 51, 10179−10190

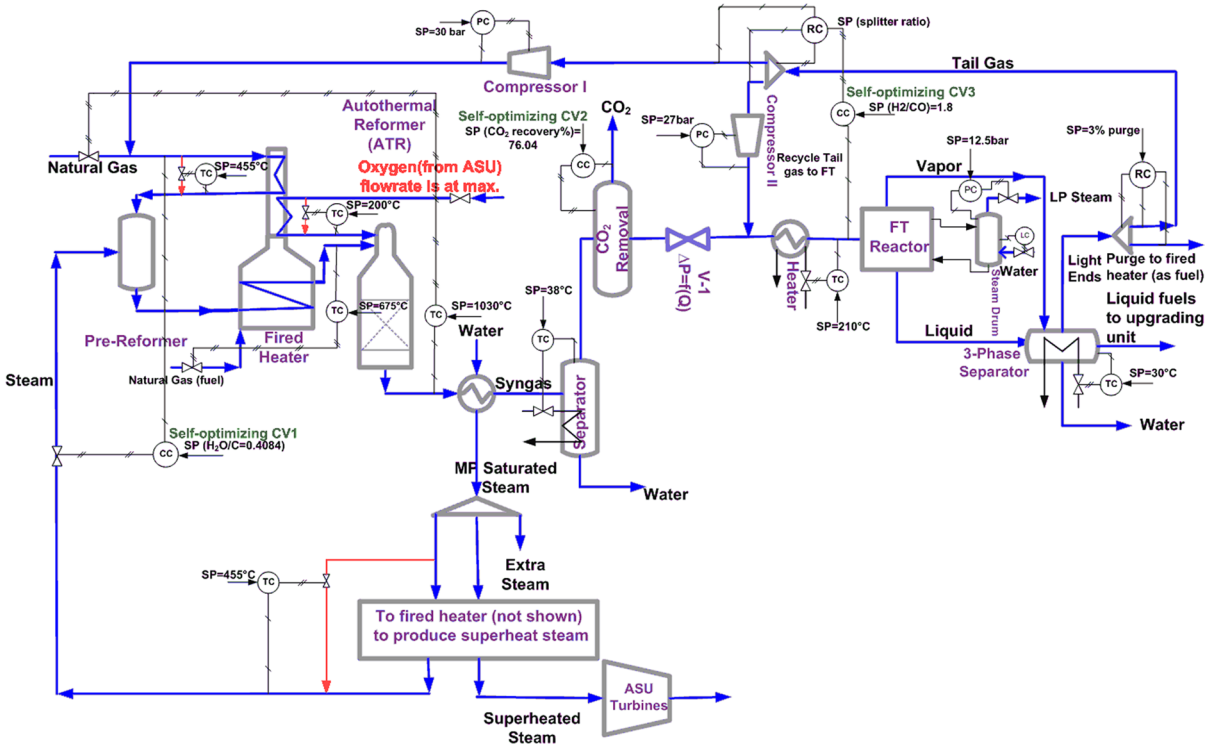

Figure 10. Possible control structure for mode II of operation.

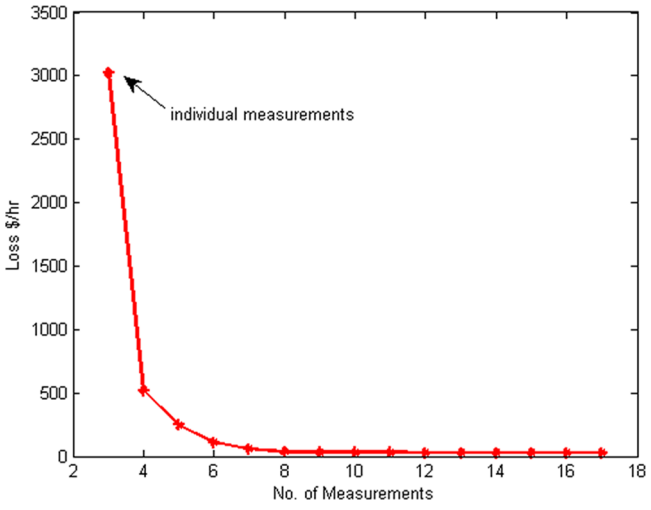

Figure 11. Minimum worst-case loss with different number of measurements (mode II).

Figure 9 shows that after saturation of oxygen capacity, as the feed natural gas feed rate increases, CO and H_2 conversions decrease and the purge flow rate and the recycle increase, all because of the constant volume of the FT reactor. This is similar to the snowballing effect,[21] which should be avoided. Therefore, the FT reactor volume may be viewed as the bottleneck of the process. Actually, the bottleneck for operation is the active constraints, but in terms of redesign it may be better to increase the reactor volume.

Unconstrained CVs in Mode II (point B). In mode II, there are 16 DOFs because the natural gas feed rate gives one extra compared to mode I. At the optimal point (point B), there are four active constraints and the same nine equality constraints as in mode I. The extra active constraint compared to mode I is the maximum oxygen flow rate. Since it then cannot be used to control the ATR exit temperature (active constraint) as we did in mode I, we select to use the natural gas feed rate to control the ATR temperature. The other pairings for control of the constraints are as for mode I. We are then again left with three unconstrained degrees of freedom which are the same as in mode I: H_2O/C, CO_2 removal percent, and recycle ratio to FT. The self-optimizing analysis is repeated to find the best set of CVs. Compared to case I, we add the maximum oxygen flow rate as a disturbance (d_8, 5%).

Individual Measurements. By applying the exact local method, we find the best individual measurements. The best five sets are presented in Table 8. In mode II, two of the unconstrained degrees of freedom are found to be self-optimizing CVs (u_1 = H_2O/C and u_2 = CO_2 removal). The best third CV is the ratio H_2/CO into the FT reactor, which should be paired with the only remaining degree of freedom, which is the recycle tail gas ratio (u_3). The resulting control structure is shown in Figure 10. Note that the objective of this work is to select controlled variables (CVs) and the shown pairings with the manipulated variables (MVs) is only a suggestion. Final pairings need to be decided and validated by using dynamic simulation, which we will consider later as our future work. By comparing the best individual measurement sets for the two modes of operation we find one common set, which is the third set in Tables 4 and 8, and interestingly, we see that two measurements, y_3 (CO_2 removal) and y_5 (H_2/CO in fresh syngas), have almost the same set point values (see the optimal values in Table 7). The set point of the third measurement, H_2O/C, changes from 0.6010 in the nominal case to 0.4084 in the optimal throughput case (point B).

In the "snowballing" region between operating points A and B, one can view the H_2O/C set point as throughput manipulator (TPM). As mentioned, from a practical point of view, it may be better to operate the plant closer to point A. This may be

dx.doi.org/10.1021/ie202678h | Ind. Eng. Chem. Res. 2012, 51, 10179−10190

Table 9. Best Set of Combination Measurements and Their Corresponding Losses in Comparison with the Best Individual Measurements Set (Mode II)

no. measurements	best set of combinatorial CVs	min worst-case loss (USD/h)
3	$CV1 = y_2$ $CV2 = y_3$ $CV3 = y_7$	3,022
4	$CV1 = 1.2265y_2 - 3.9023y_6 + 26.5645y_{11} - 44.1699y_{12}$ $CV2 = -1.4168y_2 - 3.8972y_6 + 27.4781y_{11} - 43.8481y_{12}$ $CV3 = -0.1675y_2 + 6.5306y_6 - 44.4148y_{11} + 63.5875y_{12}$	520
5	$CV1 = -3.2704y_6 - 11.0752y_{10} + 23.9689y_{11} - 39.4867y_{12} + 0.0001y_{17}$ $CV2 = -5.6662y_6 + 9.1168y_{10} + 37.8373y_{11} - 59.4219y_{12} - 0.0002y_{17}$ $CV3 = 6.1857y_6 + 0.5967y_{10} - 42.2267y_{11} + 60.4177y_{12} - 0.0000y_{17}$	153
6	$CV1 = -1.5199y_6 - 2.5054y_7 - 10.0711y_{10} + 18.6901y_{11} - 44.9909y_{12} + 14.1532y_{15}$ $CV2 = -14.6808y_6 + 15.4651y_7 + 0.8535y_{10} + 46.1202y_{11} - 11.2275y_{12} - 66.6206y_{15}$ $CV3 = 4.9366y_6 + 2.0426y_7 - 0.4327y_{10} - 40.3465y_{11} + 66.3164y_{12} - 9.4631y_{15}$	112
7	$CV1 = 4.3020y_2 + 0.7874y_3 - 3.1178y_6 + 1.4389y_7 + 12.1582y_{11} - 12.3659y_{12} - 13.6128y_{15}$ $CV2 = 0.7497y_2 + 0.2475y_3 - 13.2986y_6 + 14.2588y_7 + 39.8464y_{11} - 5.0080y_{12} - 63.7779y_{15}$ $CV3 = 0.0725y_2 + 0.0196y_3 + 5.3032y_6 + 1.5697y_7 - 41.2960y_{11} + 66.0941y_{12} - 7.6749y_{15}$	61

achieved from increasing the set point for H_2O/C from 0.4084 (point B) to 0.5357 (point A).

Measurement Combinations as CVs. As an alternative to individual measurements, we consider also combinations of CVs in mode II. Figure 11 and Table 9 illustrate the results. By combining four, five, six, and seven measurements, the worst-case loss decreases significantly to 520, 153, 112, and 61 USD/h, respectively.

4. CONCLUSIONS

The steady-state top-down part of the general plantwide control procedure was applied for selection of the best controlled variables (CVs) for a GTL process in two modes of operation. In mode I, the natural gas feed rate is given, and in mode II, the natural gas feed rate is a degree of freedom for optimization in order to achieve the maximum possible profit. The transition from mode I to mode II occurs when the oxygen flow rate reaches its maximum. In mode II, when the oxygen flow rate saturates (point A), the recycle flow rate to the FT reactor increases significantly as we further increase the feed rate toward the optimal point B. The purge flow and compressor II duty also increase. This snowballing effect should be avoided. In addition, the economic benefit of increasing the feed rate is small; therefore, it may be better in practice to operate closer toward point A.

In both mode I and mode II of operation, we have three remaining unconstrained steady-state degrees of freedom, and among the best corresponding individual measurement CV sets, we found for both modes two CVs with almost the same set point value (H_2/CO in fresh syngas and CO_2 removal percent) and a third one (H_2O/C feed) where the set point decreases from 0.6010 (nominal case) to 0.4084 (optimal throughput, point B) and this choice gives a simple transition. In mode II, the set point of the steam to carbon feed ratio (H_2O/C) can be chosen as the throughput manipulator (TPM) in the "snowballing region" between points A and B, and by reducing its value we can move closer to point A, where snowballing is avoided.

Use of combinations of measurements reduces significantly the worst-case loss. In both modes, we reach almost zero loss by combining seven measurements.

AUTHOR INFORMATION

Corresponding Author

*Tel.: +47 73594154. Fax: +47 73594080. E-mail: skoge@ntnu.no.

Notes

The authors declare no competing financial interest.

REFERENCES

(1) GTL-Workshop. Introduction to GTL Technology, Pre-Symposium Workshop; Organized by Gas Processing Center and Shell Company Doha, Qatar, 2010.

(2) Panahi, M.; Rafiee, A.; Skogestad, S.; Hillestad, M. A Natural Gas to Liquids (GTL) Process Model for Optimal Operation. *Ind. Eng. Chem. Res.* **2012**, *51* (1), 425−433.

(3) Skogestad, S. Control structure design for complete chemical plants. *Comput. Chem. Eng.* **2004**, *28* (1−2), 219−234.

(4) Rostrup-Nielsen, J.; Dybkjaer, I.; Aasberg-Petersen, K. Synthesis gas for large scale Fischer−Tropsch synthesis. *Prepr.—Am. Chem. Soc., Div. Pet. Chem.* **2000**, *45* (2), 186−189.

(5) Schanke, D.; Sogge, J. Personal communication. Statoil, Research Center, Trondheim, Norway, 2010.
(6) Aasberg-Petersen, K.; Christensen, T. S.; Stub Nielsen, C.; Dybkjær, I. Recent developments in autothermal reforming and pre-reforming for synthesis gas production in GTL applications. *Fuel Process. Technol.* **2003**, *83* (1−3), 253−261.
(7) Christensen, T. S. Adiabatic prereforming of hydrocarbons——an important step in syngas production. *Appl. Catal., A: Gen.* **1996**, *138* (2), 285−309.
(8) Aasberg-Petersen, K.; Bak Hansen, J. H.; Christensen, T. S.; Dybkjaer, I.; Christensen, P. S.; Stub Nielsen, C.; Winter Madsen, S. E. L.; Rostrup-Nielsen, J. R. Technologies for large-scale gas conversion. *Appl. Catal., A: Gen.* **2001**, *221* (1−2), 379−387.
(9) Yates, I. C.; Satterfield, C. N. Intrinsic kinetics of the Fischer−Tropsch synthesis on a cobalt catalyst. *Energy Fuels* **1991**, *5* (1), 168−173.
(10) Iglesia, E., Reyes, S. C.; Soled, S. L. Reaction-transport selectivity models and the design of Fischer-Tropsch catalysts. *Computer-Aided Design of Catalysts*; Becker, E. R., Pereira, C. J., Eds.; Marcel Dekker: New York, 1993; pp 199−257.
(11) Yermakova, A.; Anikeev, V. I. Thermodynamic Calculations in the Modeling of Multiphase Processes and Reactors. *Ind. Eng. Chem. Res.* **2000**, *39* (5), 1453−1472.
(12) Song, H.-S.; Ramkrishna, D.; Trinh, S.; Wright, H. Operating strategies for Fischer−Tropsch reactors: A model-directed study. *Korean J. Chem. Eng.* **2004**, *21* (2), 308−317.
(13) Bakkerud, P. K. Personal communication, 2009.
(14) Dybkjær, I.; Christensen, T. S.; Iglesia, J. J. S. E.; Fleisch, T. H. Syngas for large scale conversion of natural gas to liquid fuels. *Stud. Surf. Sci. Catal.* **2001**, *136*, 435−440.
(15) UniSim; UniSim Design Honeywell Co.; 2008; R380.
(16) Halvorsen, I. J.; Skogestad, S.; Morud, J. C.; Alstad, V. Optimal Selection of Controlled Variables. *Ind. Eng. Chem. Res.* **2003**, *42* (14), 3273−3284.
(17) Kariwala, V.; Cao, Y.; Janardhanan, S. Local Self-Optimizing Control with Average Loss Minimization. *Ind. Eng. Chem. Res.* **2008**, *47* (4), 1150−1158.
(18) Kariwala, V.; Cao, Y. Bidirectional branch and bound for controlled variable selection. Part II: Exact local method for self-optimizing control. *Comput. Chem. Eng.* **2009**, *33* (8), 1402−1412.
(19) Alstad, V.; Skogestad, S.; Hori, E. S. Optimal measurement combinations as controlled variables. *J. Process Control* **2009**, *19* (1), 138−148.
(20) Kariwala, V.; Cao, Y. Bidirectional Branch and Bound for Controlled Variable Selection Part III: Local Average Loss Minimization. *IEEE Trans. Ind. Inf.* **2010**, *6* (1), 54−61.
(21) Luyben, W. L. Snowball effects in reactor/separator processes with recycle. *Ind. Eng. Chem. Res.* **1994**, *33* (2), 299−305.